

ISOCAM 15 μm Search for Distant Infrared Galaxies Lensed by Clusters

Richard Barvainis

MIT Haystack Observatory, Westford, MA 01886 USA¹

Email: reb@patriot.net

Robert Antonucci

UCSB, Physics Dept., Santa Barbara, CA 93106

Email: antonucci@physics.ucsb.edu

George Helou

IPAC, 100-22, Pasadena, CA 91125

Email: gxh@ipac.caltech.edu

ABSTRACT

In a search for lensed infrared galaxies, ISOCAM images have been obtained toward the rich clusters Abell 2218 and Abell 2219 at 15 μm . Nine galaxies (four in Abell 2218 and five in Abell 2219) were detected with flux levels in the range 530–1100 μJy . Three of the galaxies detected in Abell 2218 have previously known redshifts; of these one is a foreground galaxy and the other two are lensed background galaxies at $z = 0.474$ and $z = 1.032$. One of the objects detected in the field of Abell 2219 is a faint, optically red, extreme infrared-dominated galaxy with a probable redshift of 1.048.

Subject headings: Galaxies: Clusters

1. Introduction

Clusters of galaxies can serve as windows on the distant universe by bringing faint objects above detection thresholds via gravitational lensing. Many arcs representing magnified ordinary galaxies at moderate to high redshifts are seen in rich galaxy clusters, and these have been well-studied over the past several years. Indeed some of the most distant known galaxies have been discovered in this way at optical wavelengths (see Franx et al 1997 for a lensed galaxy at $z = 4.92$). Clusters are known to be equally useful as cosmic magnifiers in other wavebands as well.

¹ Current address: 4301 Columbia Pike #610, Arlington, VA 22204

In the local universe the dominant populations of luminous objects are infrared galaxies and quasars. The ultraluminous infrared galaxies (ULIRGs), with bolometric luminosities $\gtrsim 10^{12}L_{\odot}$, appear to be powered by intense starbursts and obscured quasars (e.g., Sanders and Mirabel 1996). It remains an open question how many such objects exist among galaxy populations at high redshift, since they are obscured in the optical region and generate most of their luminosity in the mid- to far-infrared where sensitivities of space-borne telescopes such as IRAS have been marginal for their detection above redshifts of a few tenths. Indeed only one such high- z galaxy is known in the IRAS database, the infrared galaxy/hidden quasar F10214+4724, at $z = 2.3$ (Rowan-Robinson et al 1991). Two high-redshift IRAS quasars have also been identified: the Cloverleaf at $z = 2.6$, and APM 08279+5255 at $z = 3.9$, both broad absorption line quasars (Barvainis et al 1995; Irwin et al 1998). Boosting by gravitational lensing was required for the detection of F10214+4724 (Broadhurst and Lehár 1995), the Cloverleaf is a quad lens, and APM 08279+5255 appears to be a close optical double and very likely lensed as well. New lensed and unlensed infrared galaxies are currently being found via their submillimeter emission by SCUBA on the JCMT (Smail, Ivison, & Blain 1997; Ivison et al 1998; Hughes et al 1998; Barger et al 1998).

ESA’s Infrared Space Observatory (ISO) offered a new opportunity to mount systematic searches for other high- z infrared-dominated objects. The approach we adopted with ISO, which we report here, was to use the mid-infrared camera ISOCAM to image at $15 \mu\text{m}$ two very rich lensing clusters of galaxies, Abell 2218 and Abell 2219. The strategy was to enhance detectability of distant infrared galaxies over random fields by taking advantage of the cluster lensing boost. Other groups have carried out similar programs: Altieri et al (1998a) for Abell 2218; Altieri et al (1998b) and Lémonon et al (1998) for Abell 2390; and Metcalfe et al (1998) for Abell 370.

The two target clusters were chosen for their richness and for previous optical indications of lensing, along with purely observational considerations such as visibility to ISO and high ecliptic latitude. Both are at moderate redshift: $z = 0.176$ for Abell 2218, and $z = 0.225$ for Abell 2219. In this experiment several probable cluster galaxies were detected at $15 \mu\text{m}$ in the two clusters. Three background galaxies, dominated by their mid-infrared emission, were also detected. Two are previously known lensed galaxies behind Abell 2218 at redshifts $z = 0.474$ and $z = 1.034$, and the third is a faint red object in the field of Abell 2219 with a probable redshift of $z = 1.048$.

2. Observations and Data Analysis

Each cluster was observed for a total of 1.2 hours using the LW3 filter of ISOCAM covering the range $12 - 18 \mu\text{m}$. The 32×32 detector array was configured with a plate scale of $6''$ per pixel. Data were taken in “micro-scan” mode, using 3×3 rasters with $14'' = 2.33$ pixel steps to maximize the area covered and the different pixel sampling of the same sky area. Three separate such rasters, with slightly shifted centers, were taken of each cluster, to achieve yet more cross-sampling between camera pixels and sky pixels. The diffraction-limited beamsize was $6.3''$ FWHM, but with a $6''$ pixel size and multiple sampling, we estimate that the point source width should be $8 - 9''$.

There are no strong sources in the field with which to measure an accurate point spread function, but the program sources that were detected with reasonable SNR yield a FWHM of $9''$ when fitted with a circular Gaussian approximation to the PSF, or about the expected value.

For Abell 2218 the first raster was rendered unusable by detector instabilities. Only the second and third rasters were summed, for a total integration time of 0.8 hr. For Abell 2219 all three rasters were acceptable. Images were dark-subtracted, flat-fielded, deglitched, corrected for transient response, and combined using standard CIA routines at IPAC in Pasadena.

Source fluxes were derived by fitting with a circular two-dimensional Gaussian function and zero level using AIPS, with fixed FWHM of $9''$ (see above). The RMS noise levels, obtained by fitting with the same Gaussian at random points in the fields, are $\approx 200 \mu\text{Jy}$ for Abell 2218 and $\approx 110 \mu\text{Jy}$ for Abell 2219. These noise levels are well above the theoretical expectation, for reasons that are not understood by us at present; the cause is not a scaling error, since our source fluxes are consistent with those of Alieri et al (1998a) (see §3.1).

Absolute coordinates on the original ISO rasters have an uncertainty of $\sim 6''$, and small shifts were required for both ISO images to align the ISO sources with galaxies in optical frames. No rotations were required. After the shifts all of the ISO sources had clear optical identifications.

One of the detected sources in the Abell 2219 image (designated A2219#5, see below) is optically faint and very red, making it a candidate for the sort of distant infrared-dominated galaxy we were searching for. A spectrum obtained for us by T. Broadhurst and B. Frye using the Keck I telescope shows an emission line at $\lambda 7634\text{\AA}$, to which we assign a probable identification of [OII] $\lambda\lambda 3726, 3729\text{\AA}$ at $z = 1.048$. This identification is supported by the continuum shape and the lack of other strong lines in the $6300 - 9500\text{\AA}$ passband observed (see, e.g., starburst galaxy templates of Kinney et al 1996). A detection of $\text{H}\alpha$ at $1.34 \mu\text{m}$ would confirm the redshift. A possible alternative identification would be $\text{H}\alpha$ at $z = 0.163$, but we feel this is less likely than [OII] at $z = 1.048$ for the reasons given.

3. Results and Discussion

The $15 \mu\text{m}$ images are shown in Figures 1 and 2. The coordinates shown have been adjusted after comparison between the sources in the ISO image and galaxies in I-band optical images, and should be accurate to $1 - 2''$. In Abell 2218 there are four sources with detections for which we can be reasonably confident, and in Abell 2219 we identify five sources. Only detections that were evident on more than one frame are considered bona fide sources here. All of the accepted sources are closely coincident with visible-light sources. Contour overlays of the $15 \mu\text{m}$ images on I-band images from the Palomar 5m telescope are shown in Figures 3 and 4 (5m images courtesy I. Smail). An overlay of the $15 \mu\text{m}$ image of Abell 2218 on an HST R-band image is shown in Figure 5. Object identifications, with $15 \mu\text{m}$ and I-band fluxes, are given in Table 1. All sources are consistent with being point-like in the ISO images.

3.1. Detected galaxies: General discussion

Of the nine objects detected at $15\ \mu\text{m}$, three have redshifts available in the literature. These are A2218#395, #317, and #289 (using the galaxy numbering system of Le Borgne, Pello, & Sanahuja 1992; Abell 2219 has no previous numbering system and the ISO sources are numbered here according to RA order). The latter two (see §3.2) are background galaxies at $z = 0.474$ and $z = 1.034$ respectively (Ebbels et al 1997), with #289 clearly being distorted by the cluster potential. Abell 2218 has a mean redshift of 0.176 (Le Borgne et al 1992). A2218#395, at $z = 0.103$, is a foreground galaxy and not part of the cluster. As discussed above, we assign a tentative redshift of $z = 1.048$ for A2219#5.

The other detected galaxies in Abell 2218 and Abell 2219 are of unknown redshift and precise Hubble type, although the majority appear to be spirals or irregulars. None of those galaxies look particularly distorted as if by lensing, and all except A2219#5 have optical colors typical of ordinary spiral or elliptical galaxies. However, they are distinguished by their strong $15\ \mu\text{m}$ emission, which sets them apart from the hundreds of other galaxies in the ISOCAM fields.

The apparent mid-infrared luminosities (over the $\Delta\nu/\nu \sim 0.25$ of the filter passband) of the four galaxies with known redshifts, A2218#395, #317, and #289, and A2219#5, are respectively $L_{14\mu\text{m}} = 3.9 \times 10^8 L_\odot$, $L_{10\mu\text{m}} = 4.9 \times 10^9 L_\odot$, $L_{7\mu\text{m}} = 3.0 \times 10^{10} L_\odot$, and $L_{7\mu\text{m}} = 1.9 \times 10^{10} L_\odot$ (assuming $z = 1.048$ for A2219#5), where the subscripts on the luminosities represent the rest wavelengths observed. The frequency width of the $15\ \mu\text{m}$ filter has been taken to be 5.0×10^{12} Hz, and the cosmological parameters used are $H_0 = 65\ \text{km s}^{-1}\ \text{Mpc}^{-1}$ and $q_0 = 0.1$. For A2218#289 and #317, and A2219#5, the calculated luminosities represent upper limits, since the fluxes are likely to be magnified by lensing. The other galaxies, if assumed to be at the redshifts of their clusters, range in luminosity between $5.8 \times 10^8 L_\odot$ and $2.4 \times 10^9 L_\odot$. For comparison, of the 57 Virgo cluster galaxies of all Hubble types detected by Boselli et al (1998) at $15\ \mu\text{m}$, none have $L_{15\mu\text{m}}$ above $10^9 L_\odot$, and most lie in the range $10^6 - 10^8 L_\odot$. The galaxies detected here have much higher apparent luminosities in the mid-infrared than average cluster galaxies.

Boselli et al (1998) find that for spirals and irregulars the $15\ \mu\text{m}$ flux tends to be dominated by dust re-emission of primarily UV stellar light, whereas for ellipticals it is the (very weak) direct light of the Rayleigh-Jeans tail of the old population of red stars. However, for spirals the relation between star formation and $15\ \mu\text{m}$ flux is not simple. It appears that galaxies with moderate activity have the highest $15\ \mu\text{m}$ to UV flux ratios whereas for active star-forming galaxies this ratio is lower (Boselli et al 1997). The galaxies with clear spiral morphology in our sample are A2218#395 and #317, and A2219#1 and #3. A2218#289 and #275 appear irregular. The others, all in Abell 2219 (galaxies #2, #4, and #5), are difficult to classify because of lack of angular resolution (all are smaller than $3''$). However, the very small number of detections of E/SO galaxies in Virgo relative to later types by Boselli et al (1998) suggests that all or almost all of the detections here are likely to be from spirals or irregulars. This is supported by the large $15\ \mu\text{m}$ to I-band flux ratios, which are typical of spirals rather than ellipticals (see Table 1).

Altieri et al (1998a) recently reported ISOCAM imaging of Abell 2218 at 5, 7, 10, and 15 μm . Their field was roughly one-quarter the size of ours, because their pixel field of view was $3''$ compared with our $6''$. In the inner regions of the cluster they detected the central cD galaxy and five others: #395, #317, #323, #373, and #275. We detected #395, #317, #275, and possibly #373 (which we do not claim as a firm detection, although it does show up with $\sim 400 \mu\text{Jy}$ in two positive contours in Figures 4 & 5). A2218#323 is weak in Figure 2 of Altieri et al, and appears to be below our detection threshold, as does the cD galaxy. For #395 and #317 the fluxes given by Altieri et al (1998a) are consistent with ours. Our approximate flux of $\sim 400 \mu\text{Jy}$ for #373 is also consistent with the value found by Altieri et al.

3.2. Notes on individual galaxies

A2218#289, at $z = 1.034$, consists of a complex of bright knots and diffuse emission (see Figure 5). Lensing distortion is substantial at the northeastern end, where the galaxy is stretched across the halo of cluster galaxy #244; because the object appears so luminous it is probably highly magnified, according to Kneib et al (1996).

A2218#317 is a background spiral galaxy at $z = 0.474$. It is very probably magnified by the cluster, since its shape and color led to a redshift prediction by Kneib et al (1996), using cluster inversion techniques, of $0.2 < z_{\text{lensing}} < 0.4$. Given that such redshift predictions are statistical in nature, the spectroscopically measured redshift of $z = 0.474$ can be considered to be consistent with the lensing hypothesis.

A2219#5 is optically the faintest object among those detected at 15 μm , by more than an order of magnitude. It is quite red, with an optical color $B - I = 4.08$, and a 15 μm to I ratio $S_{15\mu\text{m}}/S_I = 180$; the second largest such ratio is 21 for A2218#289. A2219#5 therefore appears to be an unusual object, very red in the optical and apparently dominated in luminosity by its mid- or far-infrared emission. Lémonon et al (1998) and Altieri et al (1998b) have recently found similar objects in ISOCAM images of Abell 2390.

Referring to Figure 6, A2219#5 is well-resolved in the optical along the major axis and barely resolved along the minor axis. A 2-dimensional gaussian fit gives a FWHM size of $2.0'' \times 1.0''$ at position angle 103° (major axis). The image seeing is $\approx 0.7''$, so the deconvolved minor axis width would be $\approx 0.7''$. The direction to the center of the cluster from the location of A2219#5 lies at $\text{PA} = 210^\circ$ (see Figure 6), so the major axis is within 17° of being perpendicular to this direction, suggesting a lensed arclet.

3.3. IR/B Ratios

Table 1 lists the 15 μm -to-I ratios for all detected galaxies. The three galaxies at the highest measured redshifts have the highest ratios, as would be expected for a survey with fewer detections in the infrared than the visible. For A2218#289 and A2219#5 at redshifts near 1, the observed 15 μm /I ratio maps closely to the ratio of 7 μm /B in the rest frame. For these bands, the observed flux density ratios of 21 and 176 translate to a luminosity ratio (in νf_ν) of ~ 1 and ~ 10 .

Helou et al (1999) show that for star forming galaxies the ISO 7 μm band (5 – 9 μm) is dominated by the Aromatic features, and that the luminosity in this band accounts for 2 – 8% of the total infrared luminosity between 3 and 1000 μm . The lower luminosity fraction is characteristic of intense star bursts, while the higher fractions occur in quiescent or mildly active star forming galaxies. At the extreme luminosity and excitation end however, these fractions can drop even lower, as in Arp 220, which emits only about 0.3% of its luminosity in the 7 μm band (E. Sturm, private communication; Genzel et al. 1998). Using the higher 7 μm -to-total-IR fraction of 8% leads to IR/B ratios of 13 and 120 for A2218#289 and A2219#5, which are much higher than expected in quiescent galaxies. One is therefore led by self-consistency arguments to using a smaller fraction applicable to active galaxies. For a 7 μm -to-total-IR fraction of 2%, one finds the total IR/B ratios are ~ 40 and ~ 400 for A2218#289 and A2219#5 (extrapolating the optical spectrum to obtain B_{rest}), and the total observed IR luminosities about 1.5×10^{12} and $9.5 \times 10^{11} L_\odot$. While these are substantial luminosities, they do have to be adjusted down for gravitational lensing amplification, which is on the order of ten for A2218#289 (Casoli et al 1996), and at most a few for A2219#5 given that it is lensed by the smooth cluster potential. If A2219#5 is at a redshift of 0.163 rather than 1.048 (see §2), its luminosity would be considerably lower of course but its IR/B ratio would still be very large.

To further constrain the IR/B ratios we have analyzed the raw IRAS survey data for the best estimate of upper limits in the far-infrared, and find for each of A2218#289 and A2219#5 a three-sigma upper limit of about 225 mJy at 100 μm , in quiet sky with very little cirrus noise. This implies that the 7 μm -to-total-IR fraction must be greater than 1.6% for A2218#289, and greater than 1% for A2219#5, or they would have been detected by IRAS. These limit fractions add confidence that the 2% adopted above is a reasonably good estimate, since it is constrained from both above and below. We therefore conclude that both of the $z = 1$ objects are likely to be dusty galaxies similar to local ULIRGs, with luminosities up to a few $\times 10^{11} L_\odot$.

While IR/B ~ 40 (A2218#289) is not unusual for an active galaxy, a ratio of 400 (A2219#5) is extreme, in that it requires a high column density of gas and dust with the dust surrounding the active regions without significant leaks or clumping. Differential lensing amplification between wavelengths (Eisenhardt et al 1996) is unlikely to be the cause of the extreme ratio since A2219#5 is lensed by the diffuse potential of Abell 2219, which is too smooth to produce such an effect. Similar high ratios have been reported by Dey et al (1999) for the $z=1.44$ ERO (extremely red object) HR10 (IR/B ≈ 300), and by Yun and Scoville (1998) for IRAS F15307+3252 (IR/B

≈ 650).

A2219#5 has a number of other similarities to HR10 and other members of the ERO class, although its colors are probably not extreme enough to warrant inclusion in that class (we estimate an R–K color of 4.5, interpolating between our measured fluxes; EROs have R–K > 6). The EROs are a population of infrared bright, extremely red objects that have been discovered in near-infrared imaging surveys. Most EROs are sufficiently faint optically that their redshifts and spectral properties are unknown. The exception is HR10, for which a redshift of 1.44 has been derived based on [OII] and H α emission lines (Graham & Dey 1996; Dey et al 1999). This object is thought to be a high-redshift counterpart of the dusty, ultraluminous infrared galaxies found in the local Universe (Dey et al 1999). The optical/IR spectral energy distributions and luminosities of A2219#5 (assuming $z = 1.048$) and HR10 are similar, both are extended at the $1 - 2''$ level, and both show an emission line at long optical wavelengths, firmly identified as [OII] $\lambda\lambda 3726, 3729\text{\AA}$ in the case of HR10 and tentatively identified as the same line in A2219#5. If EROs are like A2219#5 in their infrared properties, the mid-infrared ISO detection of A2219#5 indicates that the sharply rising near-infrared spectrum of objects like HR10 continues out to at least $15 \mu\text{m}$. This is consistent with the detection of HR10 at submillimeter wavelengths by Dey et al (1999).

We conclude that the galaxies in the cluster backgrounds are luminous, high IR/B objects. As is the case for most ULIRGs, the primary driving power source, whether QSO or starburst, is unclear.

4. Summary

Nine galaxies have been detected in ISOCAM $15 \mu\text{m}$ images of the lensing clusters Abell 2218 and Abell 2219. At least three of these are luminous, high IR/B lensed background galaxies at redshifts of $0.5 - 1$, and one, behind Abell 2219, is an optically faint object heavily dominated by its mid-infrared emission. Judging from its high infrared luminosity, its high ratio of infrared to optical emission, and its red optical colors, this object appears to be active, with the source or sources of activity (starburst and/or AGN) heavily obscured by dust.

We thank Ian Smail for kindly providing optical images and photometry of the clusters, Jean-Paul Kneib for the HST image, and Tom Broadhurst and Brenda Frye for obtaining the Keck spectrum of A2219#5.

REFERENCES

- Altieri, B. et al 1998a, preprint (astro-ph/9803155)
 Altieri, B. et al 1998b, preprint (astro-ph/9808131)

- Barvainis, R., Antonucci, R., Hurt, T., Coleman, P., & Reuter, H.-P. 1995, *ApJ*, 451, L9
- Barger, A.J., et al 1998, *Nature*, 394, 248
- Boselli, A., et al 1997, *A&A*, 324, L13
- Boselli, A., et al 1998, *A&A*, 335, 53
- Broadhurst, T., & Lehár, J. 1995, *ApJ*, 450, L41
- Dey, A., Graham, J.R., Ivison, R.J., Smail, I., Wright, G.S. 1999, *ApJ*, submitted (astro-ph/9902044)
- Ebbels, T., Ellis, R., Kneib, J.-P., Le Borgne, J.-F., Pello; R., Smail, I., & Sanahuja, B. 1997, *MNRAS*, 295, 75
- Eisenhardt, P.R., Armus, L., Hogg, D.W., Soifer, B.T., Neugebauer, G., & Werner, M.W. 1976, *ApJ*, 461, 72
- Elbaz, D. 1998, to appear *Proceedings of the Special ISO Session of the IAU, Kyoto, Japan, August 1997* (astro-ph/9711348)
- Franx, M, Illingworth, G.D., Kelson, D.D., VanDokkum, P.G, & Tran, K-V 1997, *ApJ*, 486, L75
- Genzel, R., et al 1998, *ApJ*, 498, 579
- Graham, J.R., & Dey, A. 1996, *ApJ*, 471, 720
- Helou, G., et al 1999, submitted to *ApJL*
- Hughes, D., et al 1998, *Nature*, 394, 241
- Irwin, M.J., Ibata, R.A., Lewis, F.F., & Totten, E.J. 1998, *ApJ*, 505, 529
- Ivison, R.J., Smail, I., Le Borgne, J.-F., Blain, A.W., Kneib, J.-P., Bézecourt, J., Kerr, T.H., & Davies, J.K. 1998, *MNRAS*, 298, 583
- Kinney, A.L., Calzetti, D., Bohlin, R., McQuade, K., Storchi-Bergmann, T., & Schmitt, H.R. 1996, *ApJ*, 467, 38
- Kneib, J.-P., Ellis, R.S., Smail, I., Couch, W.J., & Sharples, R.M. 1996, *ApJ*, 471, 643
- Le Borgne, J.F., Pello, R., & Sanahuja, B. 1992, *A&ASupp*, 95, 87
- Lémonon, L., Pierre, M., Cesarsky, C.J., Elbaz, D., Pello; R., Soucail, G., & Vigroux, L. 1998, *A&A*, 334, 21
- Metcalfe, L. et al 1998, in "Extragalactic Astronomy in the Infrared", 1997, G.A.Mamon et al. eds (astro-ph/9803174)

Rowan-robinson, M., et al 1991, Nature, 351, 719

Sanders, D.B., & Mirabel, I.F. 1996, ARA&A, 34, 749

Smail, I., Ivison, R.J., & Blain, A.W. 1997, ApJ, 490, L5

Yun, M.S., & Scoville, N.Z. 1998, ApJ, 507, 774

FIGURE CAPTIONS

Fig. 1.— ISOCAM $15\ \mu\text{m}$ image of Abell 2218. Pixel size is $2''$, and gray scale range is -40 to $+40\ \mu\text{Jy}/\text{pixel}$. Note coordinate rotation of 40° clockwise (see tick marks). Horizontal striping near the bottom of the image is an artifact.

Fig. 2.— Same as Figure 1, for Abell 2219. Coordinate rotation 44° clockwise.

Fig. 3.— Contour overlay of ISOCAM image on I-band image from the Palomar 5-m telescope for Abell 2218. Dashed contours are negative. Contour levels: $(-3, -2, -1, 1, 2, 3, 4) \times 9\ \mu\text{Jy}$ per $2''$ pixel in original image.

Fig. 4.— Same as Figure 3, for Abell 2219. Contour levels: $(-3, -2, -1, 1, 2, 3, 4, 5, 6) \times 7\ \mu\text{Jy}$ per $2''$ pixel in original image.

Fig. 5.— Contour overlay of ISOCAM image on R-band (F702W) HST image for Abell 2218. Contours are the same as in Figure 3. For A2218#289 the centroids of the optical and infrared images differ by $< 2''$; the northwest extending lower contours for this object are caused by the image artifact noted in Figure 1. HST image courtesy J.-P. Kneib (see Kneib et al 1996)

Fig. 6.— Close-up of A2219#5 from the 5-m I-band image (Figure 4). Direction to cluster center is almost perpendicular to galaxy major axis, suggesting that this object may be a lensed arclet.

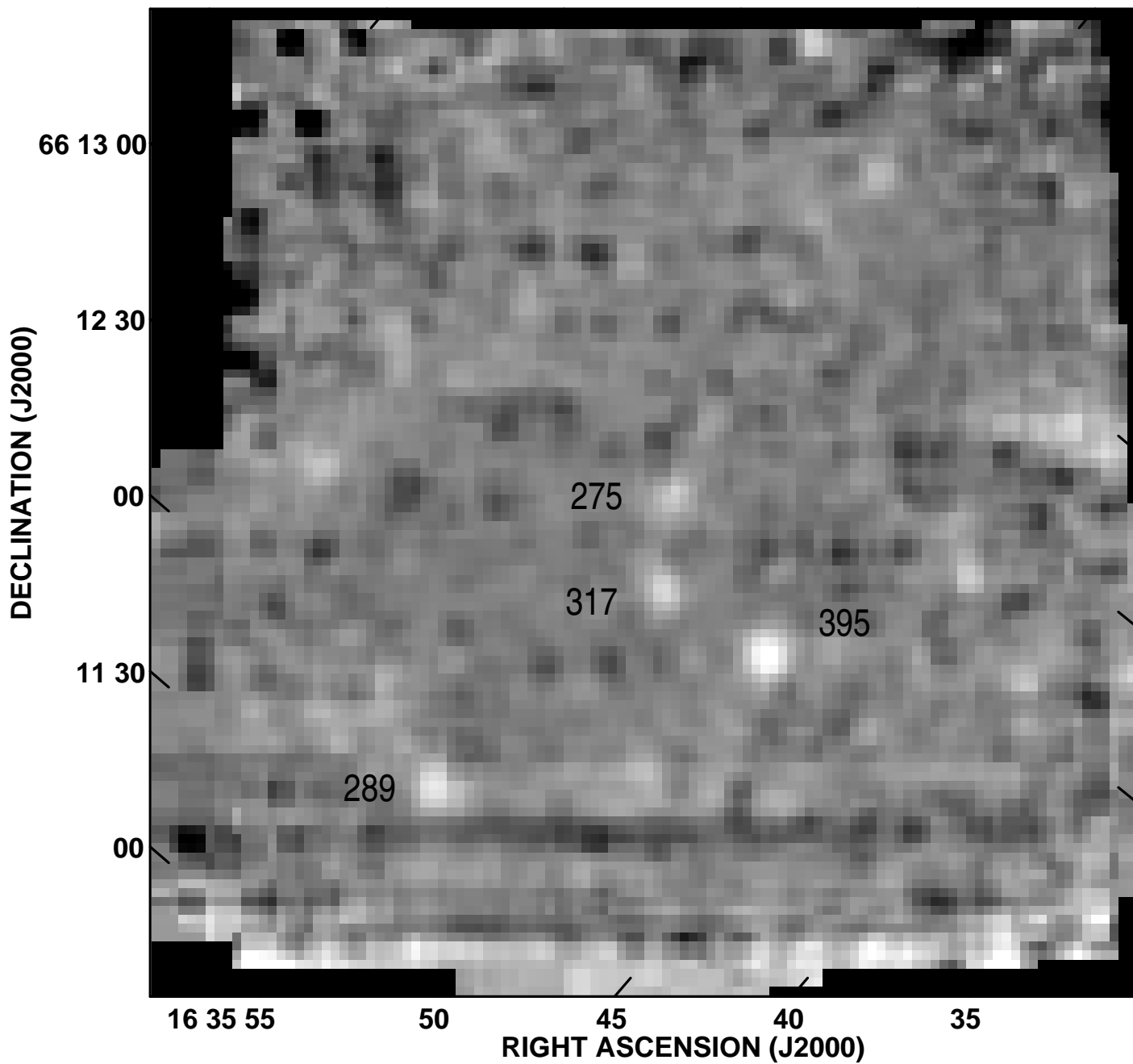
Table 1. Galaxies Detected at 15 μm

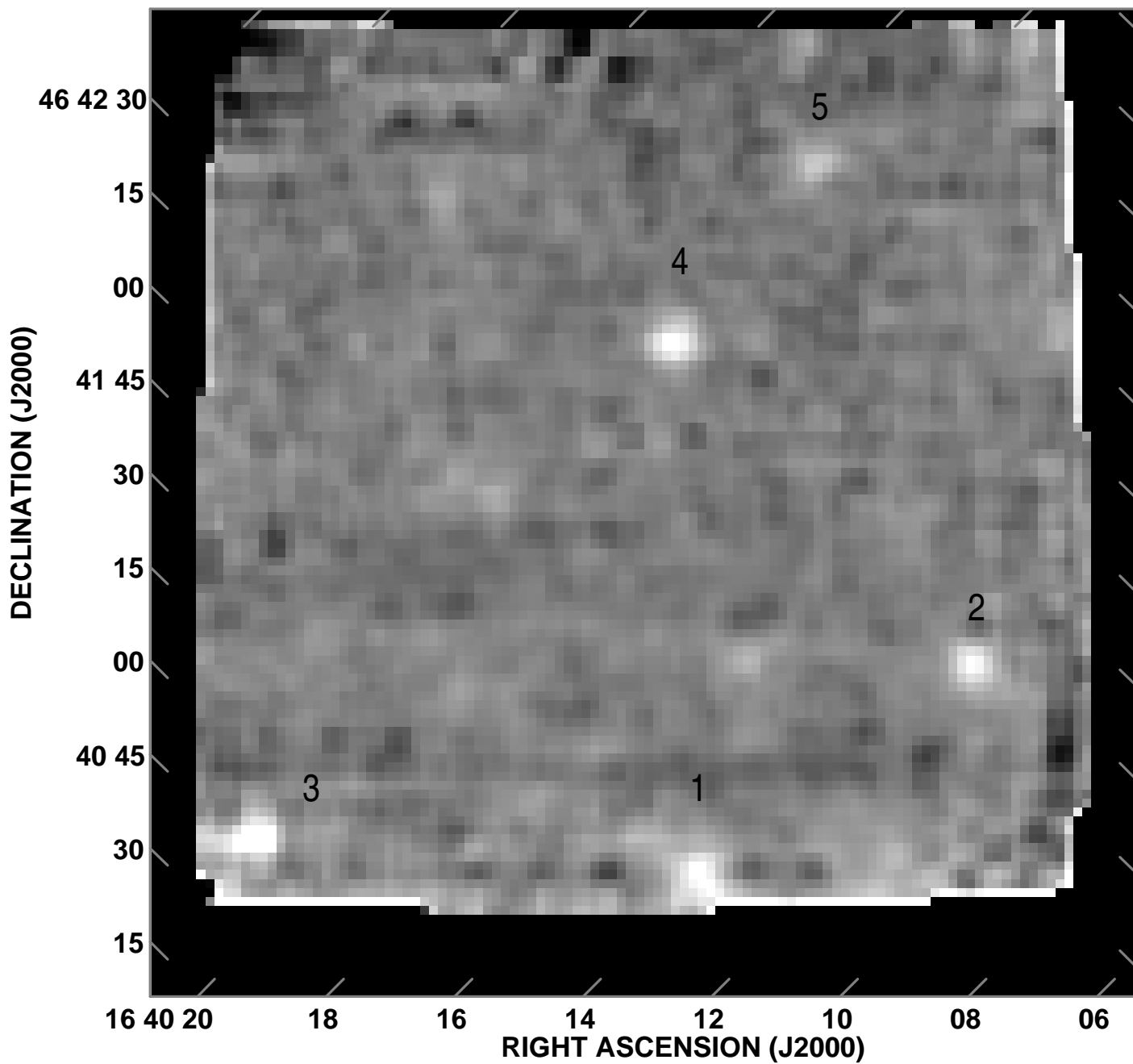
Cluster	ID ^a	RA (2000)	Dec (2000)	z^b	$S_{15\mu\text{m}}$ (μJy)	S_I^c (μJy)	S_V (μJy)	S_B (μJy)	S_U (μJy)	$B - I$ (mag)	$S_{15\mu\text{m}}/S_I$
A2218	#395	16 35 48.8	66 13 02	0.103	1100 ± 200	223	99	73	27	1.90	5
A2218	#317	16 35 53.3	66 12 58	0.474	670 ± 200	45	11	6	2	2.96	15
A2218	#289	16 35 54.8	66 11 52	1.034	850 ± 200	41	14	8	4	2.52	21
A2218	#275	16 35 55.4	66 14 15	...	570 ± 200	66	23	16	10	2.20	9
A2219	#1	16 40 13.0	46 43 07	...	890 ± 110	125	...	37	17	2.02	7
A2219	#2	16 40 13.9	46 41 51	...	920 ± 110	504	...	83	22	2.65	2
A2219	#3	16 40 21.5	46 40 49	...	1420 ± 110	201	...	40	14	2.45	7
A2219	#4	16 40 22.5	46 43 12	...	1100 ± 110	86	...	12	5	2.79	13
A2219	#5	16 40 23.0	46 44 03	1.048	530 ± 110	3	...	0.13	< 0.1	4.08	176

^aUsing numbering system of Le Borgne, Pello, & Sanahuja (1992) for Abell 2218, or RA order for Abell 2219.

^bRedshifts for objects in Abell 2218 from Ebbels et al (1997); redshift for A2219#5 is tentative, based on an emission line identified as [OII] $\lambda\lambda 3726, 3729\text{\AA}$ (see §2 of this paper).

^cIntegrated flux densities of galaxies. Estimated errors $\approx 5\%$ except for A2219#5, where the errors are 8% at I and 15% at B. For A2218#289, the photometry covers the main galaxy, and does not include the thin “tail” extending to the northeast (see Figure 5). The I -band photometry is Kron-Cousins I , with effective wavelength 8000\AA , and an assumed zero point of 2380 Janskys. The other bands are standard Johnson U, B, V . Photometry courtesy Ian Smail.





This figure "figure3.jpg" is available in "jpg" format from:

<http://arxiv.org/ps/astro-ph/9905140v1>

This figure "figure4.jpg" is available in "jpg" format from:

<http://arxiv.org/ps/astro-ph/9905140v1>

This figure "figure5.jpg" is available in "jpg" format from:

<http://arxiv.org/ps/astro-ph/9905140v1>

